first, and then the dressed nucleon propagates freely until it emits the second meson.

(c) The whole effect occurs without free propagation of the nucleon.

Just above the threshold, the relative orders in μ/M compared with the outgoing meson current term are, respectively:

(a) $O(\mu/M)$, occurring with g_s^2.

(b) $O(\mu^2/M^2)$, occurring with $g_P g_r$.

(c) $O(\mu^2/M^2)$, occurring with g_r^2.[9]

As an illustration of the determination of these relative orders, consider briefly case (b). At threshold, with zero pion mass, it contributes a term proportional to $eg_r g_P(2M)^{-2}\gamma_\mu$, since the photoproduction gives a factor $eg_P(2M)^{-1}\gamma_\mu\gamma_5$ and the remaining interaction, a factor $g_r(i\gamma p+M)^{-1}\gamma_5$, in accordance with the cancella-

---

[9] g_P is the Kroll-Rudermann constant, determined by the photoproduction of a single π meson. The relation between g_P and g_r is $g_P=(F+H)g_r$. For the definition of F and H, see reference 4, Eq. (4.3). Further, (a) has to be evaluated with care as, formally, it is infrared-divergent at threshold for $\mu=0$. In this connection, see A. Klein quoted in reference 5.

tion of the dressed propagator and vertex effects.[10] Being strictly zero at threshold, this matrix element, between $u_c^\dagger(p+\Delta p)$ and $u_c(p)$, starts with a $\Delta p/M$ factor, with increasing Δp, and its contribution is then of order $eg_r g_P(4M^3)^{-1}\mu$ just above threshold. Compared to the leading term in (2.7), this behaves just with the relative order μ^2/M^2, but with the coefficient $g_r g_P$, as stated earlier.

Thus, in conclusion, it is likely that the whole contribution to the photoproduction of two pions comes entirely from the terms of relative order k/M in (2.7) as well from the effects (b) and (c). Calculations of the effect (b) have been made, using the semiphenomenological Chew method, with results in good agreement with experiment.[11] So far, the theoretical predictions were based essentially on the perturbation expansion, giving too large an estimate owing to the pair effects. On the other hand, in the light of the present analysis, the low experimental ratio of negative to positive pions is no longer unexpected.

It is a pleasure to thank Dr. S. Deser, Dr. P. Martin, and Dr. G. Källén for many helpful discussions.

---

[10] Reference 4, Eq. (5.4).
[11] F. Zachariasen, Phys. Rev. 100, 1809(A) (1955).

High-Energy Interference Effect of Bremsstrahlung and Pair Production in Crystals*†

H. ÜBERALL
Laboratory of Nuclear Studies, Cornell University, Ithaca, New York
(Received April 13, 1956)

With the use of monocrystalline targets for bremsstrahlung and pair production experiments, interference phenomena are expected to occur which will markedly change the γ-ray spectrum as well as the pair energy distribution, for certain angles giving enhancement of radiation and pairs. The effect increases with energy; it sets in at $\delta \lesssim n_0(2\pi/a)$, where δ is the minimum momentum transfer to the target atoms, a the lattice constant, and n_0 a number of the order 2 or 3. This corresponds to $\sim$200-Mev primary energy for bremsstrahlung, $\sim$1 Bev for pair production. The effect is confined to angles between the primary beam and a line of atoms, of order $\theta \lesssim (a_{screen}/\lambda_C)(mc^2/E)$. The temperature motion of the lattice reduces the interference effect to some extent. The Born approximation was used for the quantitative analysis of the problem.

I. INTRODUCTION

IN a recent Letter to the Editor,[1] reference was made to deviations of bremsstrahlung and pair production cross sections in crystalline targets from the Bethe-Heitler formulas, and estimates of the order of magnitude of the deviations as well as the "threshold value" of primary energy were given. We here present a detailed analysis of this phenomenon.

With a classical picture of an electron passing a

---

[1] F. J. Dyson and H. Überall, Phys. Rev. 99, 604 (1955).

row of regularly spaced atoms in a lattice, it can easily be seen that, for sufficiently high speed of the electron, coherence in the successive interactions might well occur. One could expect deviations from the one-atom bremsstrahlung formula if, in the rest system of the electron, the collision frequency $c\gamma/a$ approaches the frequency of the radiation $\sim mc^2/h$. Considerations of this kind indeed led Williams[2] to surmise a corresponding interference effect for the first time.

Quantum-mechanically, such an effect should not be considered as being due to the electrons represented by waves, as their wavelength would be short compared to the lattice constant at high energies. It will rather be

---

[2] E. J. Williams, Kgl. Danske Videnskab. Selskab, Mat.-fys. Medd. 13, 4 (1935).

due to the atoms in the lattice being hit in succession, and interfering constructively by their recoil momenta which will always be small $\lesssim mc$, m being the electron mass. Similarly, one can find interference also in pair production, using the above arguments or the well-known connection between the two processes by the substitution law of the S matrix.[3] No reference is found in the literature to this effect in pair production; however, there exist some earlier theoretical papers on the bremsstrahlung interference, whose authors throughout make use of the Weizsäcker-Williams approximation. Ferretti[4] develops a formula for the radiation intensity, from which he concludes in a qualitative fashion that radiation maxima and minima should occur depending on the incidence direction of the beam with respect to the crystal, and that they should become more pronounced with increasing primary energy. These calculations were refined by Ter-Mikaelyan[5]: lattice vibrations and screening are taken into account, the position and magnitude of the diffraction maxima are calculated, and there is a careful estimation of the limits of validity of the approximations used. Both papers however present the results in a form which is not immediately useful for comparison with experiments. A step in this direction has been undertaken by Purcell,[6] who again used a Weizsäcker-Williams method. His results are in good agreement with the ones obtained below, using the Born approximation. Pair production has also been investigated by Purcell.

In the following, we shall treat the problem in Born approximation, which is expected to give more accurate results than the semiclassical Weizsäcker-Williams method, and have a wider range of applicability. Though numerical methods were used, the results are of complete generality as far as energy is concerned, but no general Z dependence can be given.

We shall present some qualitative arguments to begin with, to give an idea of the orders of magnitude involved. The essential quantity in the Born approximation matrix element of bremsstrahlung and pair production is the Fourier transform of the electrostatic potential of the nucleus,[7]

$$\int V(\mathbf{r})e^{i\mathbf{q}\cdot\mathbf{r}}d\tau, \tag{1}$$

where $\mathbf{q}$ is the momentum transfer to the nucleus. In a crystal, $V(\mathbf{r})$ will be the periodic lattice potential. In the following, we shall measure all lengths in units of the electron Compton wavelength, $\lambda_C = \hbar/mc$, and all energies and momenta (by which we mean the actual momenta times c) in units of mc^2. Moreover, we shall make the assumption throughout that mc^2 can be neglected in comparison with the energies of the electrons and quanta involved. In bremsstrahlung, we denote initial and final electron momenta and energies by $\mathbf{p}_1$, ϵ_1 and $\mathbf{p}_2$, ϵ_2, and the quantum momentum by $\mathbf{k}$. For pair production, we designate the pair by $\mathbf{p}_+$, ϵ_+ and $\mathbf{p}_-$, ϵ_-. There is always the momentum-energy relation $p^2 = \epsilon^2 - 1$.

First we shall consider the effect in momentum space, and take pair production only, the bremsstrahlung case being completely analogous. Energy and momentum conservation give the two relations

$$\mathbf{q} = \mathbf{k} - \mathbf{p}_+ - \mathbf{p}_-, \quad k = \epsilon_+ + \epsilon_-. \tag{2}$$

Taking $\mathbf{k}$ as direction of the z axis, we can show that the z component of the momentum transfer, q_z, is of order $k^{-1} \ll 1$, whereas the perpendicular component $q_\perp$ is of order 1 or smaller. To see this, we recall first that the angles of emission of the pair $\theta_\pm$ are of order $\epsilon_\pm^{-1}$. This follows immediately from the terms $\theta_\pm \epsilon_\pm (1 + \theta_\pm^2 \epsilon_\pm^2)^{-1}$ in the Bethe-Heitler formula[8] (using small-angle approximation). Now we have from (2)

$$q_z = k - p_+ \cos\theta_+ - p_- \cos\theta_-,$$

$$q_\perp^2 = p_+^2 \sin^2\theta_+ + p_-^2 \sin^2\theta_- + 2p_+ \sin\theta_+ p_- \sin\theta_- \cos\phi,$$

and expanding for small values of ϵ^{-1}, we obtain

$$q_\perp \sim 1, \quad q_z \sim 2\delta, \tag{3}$$

the indicated result. Here δ is the minimum momentum transfer, which occurs for the pair being emitted with zero angles, and which is

$$\delta = k - p_+ - p_- \approx \frac{1}{2\epsilon_+} + \frac{1}{2\epsilon_-} = \frac{k}{2\epsilon_+\epsilon_-}; \tag{4}$$

for $\epsilon_\pm \sim \frac{1}{2}k$, δ is of order k^{-1}. We also have the relations

$$q \gtrless \delta, \quad q_z \gtrless \delta, \tag{5}$$

which show that q can be of order δ to 1, q_z only of order δ. This means that pair production (and likewise bremsstrahlung) will occur predominantly in such a way that the momentum transfer to the nucleus lies in a thin, pancake-shaped region of radius 1 and thickness δ, with center shifted from the origin in $\mathbf{q}$ space along the direction of $\mathbf{k}$ (which is the axis of the pancake) by an amount δ. The momentum transfer is therefore almost completely transversal, and its magnitude is not greater than ~ 1, no matter how high the primary energy is.

In the case of a crystal potential, we can insert into (1)

$$V_{\text{cryst}} = \sum_{\mathbf{L}} V(\mathbf{r} + \mathbf{L}),$$

where V is the one-atom potential and $\mathbf{L}$ a lattice

[3] J. M. Jauch and F. Rohrlich, *The Theory of Photons and Electrons* (Addison-Wesley Press, Cambridge, 1955).
[4] B. Ferretti, Nuovo cimento **7**, 118 (1950).
[5] M. L. Ter-Mikaelyan, Zhur. Eksp. i Teort. Fiz. **25**, 296 (1953).
[6] E. M. Purcell (unpublished).
[7] W. Heitler, *The Quantum Theory of Radiation* (Oxford University Press, New York, 1954), third edition, p. 248.

[8] H. A. Bethe, Proc. Cambridge Phil. Soc. **30**, 524 (1934).

vector. So, (1) for the crystal is replaced by

$$\sum_{\mathbf{L}} \exp(i\mathbf{q}\cdot\mathbf{L}) \int V(\mathbf{r}) e^{i\mathbf{q}\cdot\mathbf{r}} d\tau,$$

which gives to the differential bremsstrahlung and pair production cross section the additional factor

$$|\sum_{\mathbf{L}} \exp(i\mathbf{q}\cdot\mathbf{L})|^2 = \frac{\sin^2(\frac{1}{2}N_1\mathbf{a}_1\cdot\mathbf{q})}{\sin^2(\frac{1}{2}\mathbf{a}_1\cdot\mathbf{q})} \frac{\sin^2(\frac{1}{2}N_2\mathbf{a}_2\cdot\mathbf{q})}{\sin^2(\frac{1}{2}\mathbf{a}_2\cdot\mathbf{q})}$$

$$\times \frac{\sin^2(\frac{1}{2}N_3\mathbf{a}_3\cdot\mathbf{q})}{\sin^2(\frac{1}{2}\mathbf{a}_3\cdot\mathbf{q})}, \quad (6)$$

a Laue-Bragg type interference factor familiar from the theory of x-ray diffraction. The $\mathbf{a}_i$ are the primitive lattice vectors and N_i the number of primitive unit cells along the ith edge of the crystal. In a non-Bravais lattice, an additional structure factor would occur also. For macroscopic crystals, the N_i are very large, and (6) can in very good approximation be written as

$$\frac{(2\pi)^3}{\Delta} N \sum_{\mathbf{g}} \delta(\mathbf{q}-2\pi\mathbf{g}), \quad (7)$$

a sum over all reciprocal lattice vectors $\mathbf{g}$, with Δ the volume of a unit cell in the lattice and N the total number of atoms in the crystal. Therefore, in a crystal, the momentum transfer has to be 2π times a reciprocal lattice vector.

To obtain the total cross section of pair production, an integration over the emission angles of the pair has to be performed. We shall see later that this can be converted into an integration over $\mathbf{q}$ space, and the main contribution will come from the pancake region. Because of (7), for a crystal this integration gets replaced by a summation of the differential cross section over the reciprocal lattice points. The situation is presented in Fig. 1 for a simple cubic lattice with lattice constant a (here the reciprocal lattice vectors coincide with the ordinary ones, only their length is changed to $1/a$). We see that for sufficiently high energies (i.e., a sufficiently thin pancake), there will be a contribution from few or many points, depending on the angle of incidence θ, and we can expect a diffraction-type variation of the cross section with θ. This instructive picture permits us to state the conditions of appearance of the effect: the thickness δ of the pancake must not be larger than the reciprocal lattice spacing to give appreciable variation of the cross section with θ, so using (4) we get

$$\delta \equiv k/2\epsilon_+\epsilon_- \lesssim 2\pi/a, \quad (8a)$$

or in the case of bremsstrahlung

$$\delta \equiv k/2\epsilon_1\epsilon_2 \lesssim 2\pi/a. \quad (8b)$$
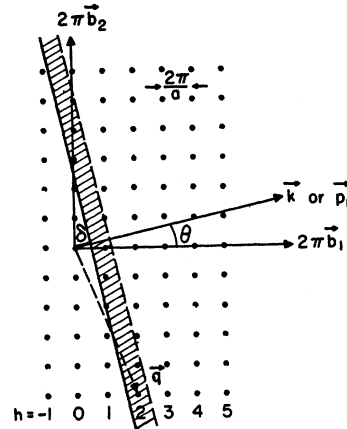
For a numerical estimate, consider a Cu target, for

FIG. 1. The "pancake" in the reciprocal lattice. $\mathbf{b}_i$ are the primitive reciprocal lattice vectors, $|\mathbf{b}_i| = 1/a$.

which $a = 3.61$ A, or $2\pi/a = 6.72\times10^{-3}$ (units mc^2). We obtain from (8a): $k \gtrsim 150$ Mev, from (8b): $\epsilon_1 \gtrsim 75$ Mev; we shall see later, however, that we have to go to somewhat higher energies in order to get more pronounced effects.

Another argument on the interference effect can be given,[9] considering the ordinary lattice space. Assume that the primary is passing a row of atoms at a small angle θ, and neglect interference from neighboring parallel rows of atoms. Then our Laue-Bragg factor is one-dimensional and simply

$$|\sum_n e^{i\mathbf{q}\cdot\mathbf{r}_n}|^2. \quad (9)$$

For small θ, we can write the phase

$$\mathbf{q}\cdot\mathbf{r}_n = na(q_z + q_\perp\theta\cos\phi);$$

this will be $\lesssim \pi$ if we have

$$n \lesssim \pi/aq_z \equiv n_0, \quad (10a)$$

$$\theta \leq \frac{\pi}{naq_\perp|\cos\phi|} \sim \frac{\pi q_z}{q_\perp}. \quad (10b)$$

With our previous estimates for q_z and q, we find that the number of lattice points over which the phase change is $\lesssim \pi$ will be of an order $n_0 \sim 3$ for pair production of ~ 1 Bev, bremsstrahlung of ~ 200 Mev, and will be larger than that at higher energies. At the same time, we see that θ has to be very small, of order $2\pi\delta$. Now (9) can be approximated by

$$|\sum_m n_0 \exp(i\mathbf{q}\cdot\mathbf{r}_{mn_0})|^2 = n_0^2 \frac{\sin^2(\frac{1}{2}N\mathbf{a}\cdot\mathbf{q})}{\sin^2(\frac{1}{2}n_0\mathbf{a}\cdot\mathbf{q})}$$

$$\approx n_0^2 \frac{N}{n_0} \frac{2\pi}{a} \sum_h \delta\left(\mathbf{q}\cdot\frac{\mathbf{a}}{a} - \frac{2\pi}{n_0 a}h\right).$$

Multiplying by the differential cross section and integrating over the angles or, equivalently, over $\mathbf{q}$,

---

[9] Based on suggestions due to Dr. Haakon Olsen.

we can replace the sum by an integral as the points h are now n_0 times closer spaced as before, and get the old one-atom cross section multiplied by n_0. This shows that an "interference length" of n_0 atoms can give constructive interference in the cross section by a factor n_0. A similar argument was used in reference 1.

Thermal motions of the lattice atoms are expected to reduce the interference effect. A particular lattice vector L will be replaced by $L+u$, where u is the displacement of the atom due to thermal vibration. The δ-function peaks of the interference factor (6) will be smoothed out if the phase change in (6) due to the displacement, $q \cdot u$, becomes of order π. Assuming[10] $\langle u \rangle \sim a/20$, we find that for $q \gtrsim q_0 = 5 \times 10^{-2}$, the interference will be markedly reduced, or in the reciprocal lattice picture, the summation over the points outside the sphere q_0 is replaced by an integration again, the sharp reciprocal lattice points being smeared out to a continuum. But as there are still about ten

reciprocal lattice points along a distance q_0, the interference effect will be reduced only partly.

II. FORMULATION OF THE PROBLEM

To obtain the total cross section in the one-atom case, the differential cross section needs to be integrated over only three variables, namely, the two emission angles of the two final particles and one relative azimuth. In the case of the crystal however, the crystal axes determine a preferential direction, and integration over two azimuths is necessary. Using the differential cross section from reference 8, we take account of this by an additional factor $(2\pi)^{-1}$. The crystal factor (6) will depend on the two azimuths separately. Table I presents our designations for the various angles.

The situation is somewhat simpler for pair production because of the symmetry between the outgoing pair particles, so let us consider this case first. We use Bethe's[8] expression for the differential cross section; after making the small-angle and high-energy approximation, it becomes

$$\sigma_{\text{pair}}\theta_+ d\theta_+ \theta_- d\theta_- d\phi_+' d\phi_+'' = \frac{-Z^2}{137}\left(\frac{e^2}{mc^2}\right)^2 \frac{\epsilon_+ \epsilon_- d\epsilon_+}{(2\pi)^2 k^3} \frac{[1-F(q)]^2}{q^4}\theta_+ d\theta_+ \theta_- d\theta_- d\phi_+' d\phi_+''$$

$$\times \left\{ 4\epsilon_+^2 \frac{\epsilon_+^2 \theta_+^2}{(1+\epsilon_+^2\theta_+^2)^2}(4\epsilon_-^2 - q^2) + 4\epsilon_-^2 \frac{\epsilon_-^2 \theta_-^2}{(1+\epsilon_-^2\theta_-^2)^2}(4\epsilon_+^2 - q^2) + 4\epsilon_+\epsilon_- \frac{2\epsilon_+\epsilon_-\theta_+\theta_- \cos\phi_+}{(1+\epsilon_+^2\theta_+^2)(1+\epsilon_-^2\theta_-^2)} \right.$$

$$\left. \times (4\epsilon_+\epsilon_- + q^2 - 2k^2) - 2k^2 \cdot 4\epsilon_+\epsilon_- \frac{\epsilon_+^2\theta_+^2 + \epsilon_-^2\theta_-^2}{(1+\epsilon_+^2\theta_+^2)(1+\epsilon_-^2\theta_-^2)} \right\}. \quad (11)$$

$F(q)$ is the atomic form factor which is calculated by Bethe using a Thomas-Fermi electron distribution. According to Schiff,[11] one can assume exponential screening as a good approximation, with a corresponding form factor

$$F(q) = 1/[1 + (qCZ^{-\frac{1}{3}})^2] \quad (12)$$

$$\sigma_{\text{pair}}(u,v,\phi_+)d\theta_+ d\theta_- d\phi_+' d\phi_+'' = \frac{-Z^2}{137(2\pi)^2}\left(\frac{e^2}{mc^2}\right)^2 \frac{16\epsilon_+\epsilon_- d\epsilon_+}{k^3} \frac{[1-F(q)]^2}{q^4}u\,du\,v\,dv\,d\phi_+' d\phi_+''$$

$$\times \left\{ \frac{(1-k\delta)q_\perp^2 + 2}{(1+u^2)(1+v^2)} - \frac{1}{(1+u^2)^2} - \frac{1}{(1+v^2)^2} \right\} \quad (13)$$

depending only on the azimuth difference ϕ_+, as the perpendicular momentum transfer is

$$q_\perp^2 = u^2 + v^2 + 2uv \cos\phi_+. \quad (14)$$

In the crystal, we have to add the factor (7) to (13). The small thickness of the pancake and the smallness of θ now permit us to replace the summation over the points in the planes perpendicular to b_1 by an integration over these planes. This will be a very good approximation indeed for angles of order given by Eq. (10b),

and an adjusted parameter $C = 111$; we shall later designate $CZ^{-\frac{1}{3}} = \beta$. This quantity approximately represents the screening radius $a_{\text{screen}} = 137Z^{-\frac{1}{3}}$.

We introduce new variables $u = \theta_-\epsilon_-$, $v = \theta_+\epsilon_+$, in which the Bethe-Heitler differential cross section takes on the simple form

because the pancake then contains a large number of atoms of a given plane. Then we can use

$$\frac{2\pi}{a}N \sum_h \delta\left(q \cdot \frac{a_1}{a} - \frac{2\pi}{a}h\right) \quad (15)$$

instead of (7). In the ordinary lattice space, this corresponds to replacing the actual crystal also by a set of smoothed-out continuous planes such that the primary direction forms the angle θ with the normals of the planes. This sheds light on the usefulness of our one-dimensional lattice-space argument of Sec. I.

[10] P. P. Ewald, Handbuch der Physik (Verlag Julius Springer, Berlin, 1933), Part 2, Vol. 23.
[11] L. I. Schiff, Phys. Rev. 83, 252 (1951).

At this point, other lattice structures besides the simple cubic lattices considered above might be investigated. Take a face-centered-cubic lattice (e.g., Cu, Pt) with lattice constant $a=$ edge of fundamental cube. The reciprocal lattice is body-centered cubic, its fundamental cube having an edge $2/a$. When we replace the lattice planes perpendicular to $\mathbf{b}_1$ by smoothed out planes, the plane nearest to the one containing the origin will be the one containing the center point of the fundamental cube; so we have a spacing of the planes of $1/a$, and get exactly the same situation as if we had taken a simple cubic lattice with lattice constant a. In fact, any lattice with a cubic basis produces the same interference effect as a simple cubic lattice. This is found to be true even for such complex cubic structures as the diamond lattice.

We now evaluate the relevant quantity in (15) in our new variables:

$$\mathbf{q} \cdot \frac{\mathbf{a}_1}{a} = \frac{\mathbf{a}_1}{a} \cdot (\mathbf{k} - \mathbf{p}_+ - \mathbf{p}_-) = k \cos\theta - p_+ \cos\theta_2 - p_- \cos\theta_1$$

$$\approx \delta - \tfrac{1}{2}(k\theta^2 - p_+\theta_2^2 - p_-\theta_1^2).$$

The angles in Table I(a) satisfy

$$\theta_1^2 = \theta_-^2 + \theta^2 - 2\theta_-\theta \cos\phi_+'', \quad \theta_2^2 = \theta_+^2 + \theta^2 - 2\theta_+\theta \cos\phi_+',$$

and we obtain

$$\mathbf{q} \cdot \frac{\mathbf{a}_1}{a} = q_z - \theta(u \cos\phi_+'' + v \cos\phi_+'), \qquad (16)$$

where we have introduced the longitudinal momentum transfer, which is in our new variables

$$q_z = k - p_+ \cos\theta_+ - p_- \cos\theta_- \approx \delta + \frac{u^2}{2\epsilon_-} + \frac{v^2}{2\epsilon_+}. \quad (17)$$

As the differential cross section depends only on ϕ_+, we shall in the integration of (13) with the factor (15) go over from the variables ϕ_+', ϕ_+'' to ϕ_+, ϕ_+'' and perform the ϕ_+'' integration with the help of the δ function. The result of this integration on (15) is

$$\begin{cases} \dfrac{2\pi}{a} N \sum_h \dfrac{2}{[\theta^2 q_\perp^2 - (q_z - 2\pi h/a)^2]^{\frac{1}{2}}} \\ \qquad\qquad\qquad \text{for } |q_z - 2\pi h/a| < \theta q_\perp, \quad (18) \\ 0 \qquad\qquad\qquad \text{for } |q_z - 2\pi h/a| \geqslant \theta q_\perp. \end{cases}$$

In place of the variable ϕ_+, we introduce $q_\perp^2$ by the relation (14). We have now a Jacobian

$$\frac{\partial(\theta_+, \theta_-, \phi_+)}{\partial(u, v, q_\perp^2)} = \frac{1}{\epsilon_+ \epsilon_- [4u^2 v^2 - (u^2 + v^2 - q_\perp^2)^2]^{\frac{1}{2}}}, \quad (19)$$

(a) Pair production	(b) Bremsstrahlung	
$\theta = \measuredangle(\mathbf{k}, \mathbf{a}_1)$	$\theta = \measuredangle(\mathbf{p}_1, \mathbf{a}_1)$	
$\theta_{12} = \measuredangle(\mathbf{p}_{-+}, \mathbf{a}_1)$	$\theta_2 = \measuredangle(\mathbf{p}_2, \mathbf{a}_1)$ $\Theta_{12} = \measuredangle(\mathbf{p}_{12}, \mathbf{k})$	
$\theta_{\pm} = \measuredangle(\mathbf{p}_{\pm}, \mathbf{k})$	$\theta_3 = \measuredangle(\mathbf{k}, \mathbf{a}_1)$ $\Theta_3 = \measuredangle(\mathbf{p}_1, \mathbf{p}_2)$	
$\phi_+' = \measuredangle(\mathbf{p}_+\mathbf{k} \text{ plane}, \mathbf{a}_1\mathbf{k} \text{ plane})$	$\psi_1 = \measuredangle(\mathbf{p}_1\mathbf{k} \text{ plane}, \mathbf{p}_1\mathbf{a}_1 \text{ plane})$	
$\phi_+'' = \measuredangle(\mathbf{p}_-\mathbf{k} \text{ plane}, \mathbf{a}_1\mathbf{k} \text{ plane})$	$\psi_3 = \measuredangle(\mathbf{p}_1\mathbf{p}_2 \text{ plane}, \mathbf{p}_1\mathbf{a}_1 \text{ plane})$	
$\phi_+ = \phi_+' - \phi_+''$	$\phi_{12} = \measuredangle(\mathbf{p}_{12}\mathbf{k} \text{ plane}, \mathbf{a}_1\mathbf{k} \text{ plane})$	
	$\psi = \psi_3 - \psi_1$	

and the total pair-production cross section has the simple form

$$\sigma_{t,\text{pair}} = N \sum_h \int' 2\pi\sigma_{\text{pair}} \frac{\partial(\theta_+, \theta_-, \phi_+)}{\partial(u, v, q_\perp^2)}$$

$$\times du\, dv\, dq^2 \frac{2}{a[\theta^2 q_\perp^2 - (q_z - 2\pi h/a)^2]^{\frac{1}{2}}}, \quad (20)$$

with (13) and (19). The prime on the integral sign indicates that we must integrate over those regions only for which the radical in (20) is real. If the last factor in the integrand were absent, we would get exactly the one-atom formula multiplied by N. The expression contains the one-atom formula as a limiting case if the lattice constant a goes to infinity. For large a's, a step from h to $h+1$ in the sum will change the integrand very little, so that we may replace $\sum_h \to \int dh$, and the last factor integrates out to 1, leaving us exactly with N times the Bethe-Heitler cross section, as it should.

To carry the integration one step further, new variables x and $y \equiv q_z - \delta$ will be introduced instead of u and v by the equations

$$u^2 = \frac{x}{2\delta\epsilon_+} + \frac{y}{\delta} + q_\perp^2 \frac{\epsilon_- - \epsilon_+}{2\epsilon_+ k\delta},$$

$$v^2 = \frac{-x}{2\delta\epsilon_-} + \frac{y}{\delta} + q_\perp^2 \frac{\epsilon_+ - \epsilon_-}{2\epsilon_- k\delta},$$

$$(21)$$

the coefficients are chosen such that the expression in the square root of (19) becomes simply

$$4u^2 v^2 - (u^2 + v^2 - q_\perp^2)^2 = w^2 - x^2, \quad (22)$$

with

$$w^2 = \frac{4q_\perp^2}{\delta} y - \frac{2q_\perp^4}{k\delta}.$$

The integrals over x can then be performed analytically. The limits of integration for both u and v were 0 and ∞, and 0 and 2π for ϕ_+. Expressing ϕ_+ by $q_\perp^2$, we let $q_\perp^2$ go from 0 to ∞ and take the result with a factor two, because when ϕ_+ covers its complete range, $q_\perp^2$ covers its range twice. In the new variables, the limits on x are given automatically by the zeros of the expression (22) whose root appears in the Jacobian, and are $\pm w$. For

the same reason, the limits on q_z are $\delta + q_\perp^2/2k$ and, of course, q. After the x-integration, the cross section becomes

$$\sigma_{t,\,\text{pair}} = \frac{-Z^2}{137}\left(\frac{e^2}{mc^2}\right)^2 \frac{8N}{a} \frac{\epsilon_+\epsilon_- d\epsilon_+}{k^3} \sum_h \int_0^\infty dq_\perp^2 \int_{\delta+q_\perp^2/2k}^{'q} \frac{[1-F(q)]^2}{q^4}$$

$$\times \frac{dq_z}{\left[\theta^2 q_\perp^2 - \left(q_z - \frac{2\pi}{a}h\right)^2\right]^{\frac{1}{2}}} \left\{ -\delta \frac{q_z + q^2_\perp[(\epsilon_- - \epsilon_+)/2\epsilon_+ k]}{\left[\left(q_z - \frac{q_\perp^2}{2\epsilon_+}\right)^2 + \frac{q_\perp^2}{\epsilon_+^2}\right]^{\frac{3}{2}}} - \delta \frac{q_z + q_\perp^2[(\epsilon_+ - \epsilon_-)/2\epsilon_- k]}{\left[\left(q_z - \frac{q_\perp^2}{2\epsilon_-}\right)^2 + \frac{q_\perp^2}{\epsilon_-^2}\right]^{\frac{3}{2}}} \right.$$

$$\left. + [(1-k\delta)q_\perp^2 + 2]\left[\frac{1}{2\epsilon_+ q_z} \frac{1}{\left[\left(q_z - \frac{q_\perp^2}{2\epsilon_+}\right)^2 + \frac{q_\perp^2}{\epsilon_+^2}\right]^{\frac{1}{2}}} + \frac{1}{2\epsilon_- q_z} \frac{1}{\left[\left(q_z - \frac{q_\perp^2}{2\epsilon_-}\right)^2 + \frac{q_\perp^2}{\epsilon_-^2}\right]^{\frac{1}{2}}} \right] \right\}. \quad (23)$$

The formula shows the desired symmetry between positron and electron, but is otherwise rather complicated. All these derivations were made for a crystal with rigid atoms; we shall see later that the inclusion of thermal motion will simplify matters. Before that, however, let us derive the corresponding formulas for bremsstrahlung.

The angular situation is somewhat more complicated here [Table I (b)], because the primary is now the electron p_1, whereas the differential Bethe-Heitler formula depends on the azimuth difference ϕ, measured from the direction of the quantum k as axis. Having the preference direction a_1, we cannot integrate over the electron angles, as Bethe[8] did, but have to keep p_1 fixed with respect to a_1.

Again using small-angle and high-energy approximation, the differential cross section[8] becomes

$$\sigma_{\text{br}}\Theta_1 d\Theta_1 \Theta_2 d\Theta_2 d\phi_1 d\phi_2 = \frac{Z^2}{137}\left(\frac{e^2}{mc^2}\right)^2 \frac{\epsilon_2 dk}{(2\pi)^2 \epsilon_1 k} \frac{[1-F(q)]^2}{q^4} \Theta_1 d\Theta_1 \Theta_2 d\Theta_2 d\phi_1 d\phi_2$$

$$\times \left\{ 4\epsilon_2^2 \frac{\epsilon_2^2\Theta_2^2}{(1+\epsilon_2^2\Theta_2^2)^2}(4\epsilon_1^2 - q^2) + 4\epsilon_1^2 \frac{\epsilon_1^2\Theta_1^2}{(1+\epsilon_1^2\Theta_1^2)^2}(4\epsilon_2^2 - q^2) - 4\epsilon_1\epsilon_2 \frac{2\epsilon_1\epsilon_2\Theta_1\Theta_2\cos\phi}{(1+\epsilon_1^2\Theta_1^2)(1+\epsilon_2^2\Theta_2^2)} \right.$$

$$\left. \times (4\epsilon_1\epsilon_2 - q^2 + 2k^2) + 2k^2 \cdot 4\epsilon_1\epsilon_2 \frac{\epsilon_1^2\Theta_1^2 + \epsilon_2^2\Theta_2^2}{(1+\epsilon_1^2\Theta_1^2)(1+\epsilon_2^2\Theta_2^2)} \right\}. \quad (24)$$

Energy and momentum conservation now make

$$k = \epsilon_1 - \epsilon_2, \quad \mathbf{q} = \mathbf{p}_1 - \mathbf{p}_2 - \mathbf{k}.$$

To keep the incoming electron momentum p_1 fixed, we shall integrate over the angles of p_2 and the quantum, $\Theta_1\Theta_3\psi_1\psi_3$, and accordingly have to take the element of solid angle

$$\Theta_1 d\Theta_1 \Theta_3 d\Theta_3 d\psi_1 d\psi_3$$

rather than the one used in (24). To express the Bethe-Heitler cross section in these angles, we find by

spherical trigonometry:

$$\Theta_2^2 = \Theta_1^2 + \Theta_3^2 - 2\Theta_1\Theta_3\cos\psi,$$

with $\psi = \psi_3 - \psi_1$, and using $\Theta_1^2 + \Theta_2^2 - 2\Theta_1\Theta_2\cos\phi = \Theta_3^2$, we have furthermore

$$2\Theta_1\Theta_2\cos\phi = 2(\Theta_1^2 - \Theta_1\Theta_3\cos\psi).$$

We now introduce new variables $u = \Theta_1 k$, $v = \Theta_3\epsilon_2$, in which the perpendicular momentum transfer (perpendicular with respect to p_1 as the z axis) takes its former simple form

$$q_\perp^2 = u^2 + v^2 + 2uv\cos\psi, \quad (25)$$

and the Bethe-Heitler formula becomes

$$\sigma_{\text{br}}(u,v,\psi)d\Theta_1 d\Theta_3 d\psi_1 d\psi_3 = \frac{Z^2}{137}\left(\frac{e^2}{mc^2}\right)^2 \frac{16\epsilon_1\epsilon_2 k dk}{(2\pi)^2} \frac{[1-F(q)]^2}{q^4} u du v dv d\psi_1 d\psi_3$$

$$\times \left\{ -\frac{1}{(k^2 + \epsilon_1\epsilon_2 u^2 + \epsilon_1 k v^2 - \epsilon_2 k q_\perp^2)^2} - \frac{1}{(k^2 + \epsilon_1^2 u^2)^2} + \frac{(1+k\delta)q_\perp^2 + 2}{(k^2 + \epsilon_1\epsilon_2 u^2 + \epsilon_1 k v^2 - \epsilon_2 k q_\perp^2)(k^2 + \epsilon_1^2 u^2)} \right\}. \quad (26)$$

The crystal factor is (15), as before, and its argument now becomes

$$\mathbf{q} \cdot \frac{\mathbf{a}_1}{a} = \frac{\mathbf{a}_1}{a} \cdot (\mathbf{p}_1 - \mathbf{p}_2 - \mathbf{k}) = p_1 \cos\theta - p_2 \cos\theta_2 - k \cos\theta_3$$

$$\approx \delta - \tfrac{1}{2}(p_1\theta^2 - p_2\theta_2{}^2 - k\theta_3{}^2) = q_z - \theta(u \cos\psi_1 + v \cos\psi_3); \quad (27)$$

the last equation was obtained by using

$$\theta_2{}^2 = \theta^2 + \Theta_3{}^2 - 2\theta\Theta_3 \cos\psi_3, \quad \theta_3{}^2 = \theta^2 + \Theta_1{}^2 - 2\theta\Theta_1 \cos\psi_1,$$

and introducing the momentum transfer along $\mathbf{p}_1$:

$$q_z = p_1 - p_2 \cos\Theta_3 - k \cos\Theta_1 \approx \delta + \frac{u^2}{2k} + \frac{v^2}{2\epsilon_2}. \quad (28)$$

Again we go over to azimuths ψ, ψ_1, and integrate over ψ_1 with the help of the δ function; this replaces the crystal factor (15) as before by (18). Elimination of the variable ψ in favor of $q_\perp{}^2$ gives the Jacobian

$$\frac{\partial(\Theta_1, \Theta_3, \psi)}{\partial(u, v, q_\perp{}^2)} = \frac{1}{\epsilon_2 k[4u^2v^2 - (u^2 + v^2 - q_\perp{}^2)^2]^{\frac{1}{2}}}, \quad (29)$$

and we obtain for the total cross section once more

$$\sigma_{t,\mathrm{br}} = N \sum_h \int' 2\pi\sigma_{\mathrm{br}} \frac{\partial(\Theta_1, \Theta_3, \psi)}{\partial(u, v, q_\perp{}^2)}$$

$$\times du\, dv\, dq_\perp{}^2 \frac{2}{a\left[\theta^2 q_\perp{}^2 - \left(q_z - \frac{2\pi}{a}h\right)^2\right]^{\frac{1}{2}}}, \quad (30)$$

with (26) and (29). Now we introduce x and $y \equiv q_z - \delta$ by the relations

$$u^2 = \frac{k}{\epsilon_1}x + \frac{2\epsilon_2 k}{\epsilon_1}y + q_\perp{}^2 k\frac{k - \epsilon_2}{\epsilon_1{}^2},$$

$$\qquad\qquad\qquad\qquad\qquad\qquad (31)$$

$$v^2 = -\frac{\epsilon_2}{\epsilon_1}x + \frac{2\epsilon_2 k}{\epsilon_1}y + q_\perp{}^2 \epsilon_2 \frac{\epsilon_2 - k}{\epsilon_1{}^2}.$$

They make the square root in (29) become $w^2 - x^2$ again, with

$$w^2 = 8\frac{\epsilon_2{}^2 k}{\epsilon_1}q_\perp{}^2 y - \frac{4\epsilon_2 k}{\epsilon_1{}^2}q_\perp{}^4. \quad (32)$$

The limits on q_z become $\delta + q_\perp{}^2/2\epsilon_1$ and q, and the resulting total cross section is after analytic x-integration:

$$\sigma_{t,\mathrm{br}} = \frac{Z^2}{137}\left(\frac{e^2}{mc^2}\right)^2 \frac{4N}{a} \frac{dk}{\epsilon_1{}^2} \sum_h \int_0^\infty dq_\perp{}^2 \int_{\delta + q_\perp{}^2/\epsilon_1}^{'q} \frac{[1 - F(q)]^2}{q^4} \frac{dq_z}{[\theta^2 q_\perp{}^2 - (q_z - 2\pi h/a)^2]^{\frac{1}{2}}}$$

$$\times \left\{ -\frac{1}{(q_z - q_\perp{}^2/2\epsilon_1)^2} - \frac{q_z + q_\perp{}^2(k - \epsilon_2)/2\epsilon_1\epsilon_2}{[(q_z - q_\perp{}^2/2\epsilon_2)^2 + 4\delta^2 q_\perp{}^2]^{\frac{3}{2}}} + \frac{(1 + k\delta)q_\perp{}^2 + 2}{q_z - q_\perp{}^2/2\epsilon_1} \frac{1}{[(q_z - q_\perp{}^2/2\epsilon_2)^2 + 4\delta^2 q_\perp{}^2]^{\frac{1}{2}}} \right\}. \quad (33)$$

It might be noted that the limit of the q_z integral shows us that the left boundary of the pancake, Fig. 1, is sharp and slightly paraboloidally shaped. The right boundary is not sharp.

Formulas (23) and (33) are valid for a "perfect" crystal whose atoms form a rigid lattice. In the next section, we shall consider the influence of zero-point and temperature oscillations of the atoms.

III. EFFECT OF LATTICE VIBRATIONS

We consider the atom at $\mathbf{L}$ to be displaced by a small amount $\mathbf{u}_L$. If we assume that the electron configuration does not get distorted thereby, we obtain a new diffraction factor instead of (6):

$$|\sum_L \exp[i\mathbf{q} \cdot (\mathbf{L} + \mathbf{u}_L)]|^2. \quad (34)$$

$\mathbf{u}_L$ can be expressed by the normal coordinates of the lattice,[12] and (34) averaged over the distribution of normal coordinates at a given temperature T, using the oscillator distribution function of Bloch.[13] Then we approximate in the usual way the Brillouin zone by

a sphere of equivalent volume, replace the sum over the Brillouin zone by an integral, and introduce the Debye temperature by

$$\omega_{\max} \equiv 2\pi(3/4\pi a^3)^{\frac{1}{3}}v = k\Theta/\hbar.$$

The frequency of lattice vibrations ω has been put equal to vq, with the sound velocity v independent of polarization. Thus we obtain

$$\langle |\sum_L \exp[i\mathbf{q} \cdot (\mathbf{L} + \mathbf{u}_L)]|^2 \rangle$$

$$= \sum_{L,L'} \exp\left[i\mathbf{q} \cdot (\mathbf{L} - \mathbf{L}') + Aq^2\left(\frac{\sin^2\alpha|\mathbf{L} - \mathbf{L}'|}{\alpha^2|\mathbf{L} - \mathbf{L}'|^2} - 1\right) \right], \quad (35)$$

calling

$$A = \frac{3m^2c^2}{4Mk\Theta}\left[1 + 4\frac{T}{\Theta}\Phi\left(\frac{\Theta}{T}\right)\right], \quad \alpha = \frac{\pi}{a}\left(\frac{3}{4\pi}\right)^{\frac{1}{3}}. \quad (36)$$

Here $\Phi(\Theta/T)$ is a function tabulated by Debye.[10] Strictly speaking, (35) was derived by us only for the case $T = 0$, as the Bloch distribution function is then especially simple. The general expression for A has then been obtained by comparison of (35) with the expression derived by Debye[10] in place of (35), which is

$$\exp(-Aq^2)|\sum_L \exp(i\mathbf{q} \cdot \mathbf{L})|^2 + N[1 - \exp(-Aq^2)]. \quad (37)$$

[12] F. Seitz, *The Modern Theory of Solids* (McGraw-Hill Book Company, Inc., New York, 1940).
[13] F. Bloch, Z. Physik **74**, 295 (1932).

TABLE II. Atomic constants of selected elements.

Element	Z	Θ	M/m_H	$a[A]$	Lattice	$A(0)/(137Z^{-\frac{1}{3}})^2$	$A(0)$	$A(77)/A(0)$[a]	$A(293)/A(0)$
Diamond	6	1860	12.01	3.56	diam	1.907×10^{-2}	108.4	1.0135	1.1916
Cu	29	315	63.57	3.61	fcc	6.090×10^{-2}	121.1	1.3745	$\cdots$
Pt	78	225	195.23	3.92	fcc	5.370×10^{-2}	55.2	1.6735	$\cdots$

[a] Liquid-nitrogen temperature.

In x-ray diffraction, this gives rise to a Laue-Bragg term in the scattered intensity, reduced by the Debye-Waller factor,[10] and an additional background scattering which is continuous in angle. Waller later showed that Debye's derivation of (37) was wrong as he obtained the second term by treating the atoms as independent oscillators, but we shall see that we can use (37) with an accuracy sufficient for our purposes. The usual treatment in x-ray diffraction theory[14] consists of an expansion of the second exponential in (35) (except for the Debye-Waller factor). This is not possible in our case, however, as we have to do with much larger q values. But the shape of the function $\sin^2 x/x^2$ in the exponential suggests to treat the term $L = L'$ separately, so that we obtain from (35):

$$N + \sum_{L,L'}{}' \exp\left[i\mathbf{q}\cdot(L-L') + Aq^2\left(\frac{\sin^2(\alpha|L-L'|)}{\alpha^2|L-L'|^2}-1\right)\right].$$

Now for $L \neq L'$, we have $|L-L'| \geqslant a$, and are therefore well outside the principal maximum of the function $\sin^2 x/x^2$ (using A- values from Table II). The side-maxima are not longer than 0.05, so that we can neglect $\sin^2(\alpha|L-L'|)/\alpha^2|L-L'|^2$ in the exponent compared to 1. This leads to the old Debye expression (37).

The interference effect will be least disturbed in elements for which the ratio of the mean temperature displacement (given by $A^{\frac{1}{2}}$) to the screening radius $137Z^{-\frac{1}{3}}$ is smallest. For three elements satisfying this condition, the atomic constants are listed in Table II.

If we now use the crystal factor (37), we shall get the following results. The second term gives a contribu-
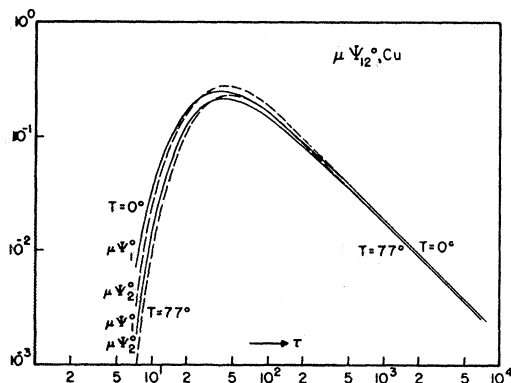
FIG. 2. $\mu\Psi_{12}^0$ for Cu as functions of $\tau = \theta/\delta$.

[14] R. W. James, *Optical Principles of X-ray Diffraction* (G. Bell and Sons, London, 1953).

tion to the cross section which is similar to the one-atom cross section, as it does not depend on θ. It is analogous to the continuous x-ray diffraction background. We can simply obtain this part of the cross section by introducing the factor

$$N[1- \exp(-Aq^2)]$$

into Bethe's[8] formula (B 50) which represents the cross section as an integral over q; comparison with the derivation of (B 50) show that this procedure is justified if we use values of A given in Table II. Thus we can represent the continuous term of the cross section as follows:

$$\sigma_{t,\,\mathrm{pair}}{}^C = N\frac{Z^2}{137}\left(\frac{e^2}{mc^2}\right)^2\frac{d\epsilon_+}{k^3}$$

$$\times[(\epsilon_+^2+\epsilon_-^2)\Psi_1{}^C(\delta)+\tfrac{2}{3}\epsilon_+\epsilon_-\Psi_2{}^C(\delta)], \quad (38)$$

$$\sigma_{t,\,\mathrm{br}}{}^C = N\frac{Z^2}{137}\left(\frac{e^2}{mc^2}\right)^2\frac{dk}{k\epsilon_1^2}$$

$$\times[(\epsilon_1^2+\epsilon_2^2)\Psi_1{}^C(\delta)-\tfrac{2}{3}\epsilon_1\epsilon_2\Psi_2{}^C(\delta)]. \quad (38')$$

In both cases, the same functions $\Psi_{12}{}^C$ appear. They depend on the δ's of the respective processes only, not on θ, and therefore represent an isotropic contribution to the cross section. The Z dependence cannot be given generally, as it was possible in the one-atom case. The $\Psi_{12}{}^C$ are given by

$$\Psi_1{}^C(\delta) = 4+4\int_\delta^1 [1-\exp(-Aq^2)](q-\delta)^2[1-F(q)]^2\frac{dq}{q^3},$$

$$\Psi_2{}^C(\delta) = \frac{10}{3}+4\int_\delta^1 [1-\exp(-Aq^2)]\left(q^3-6\delta^2 q\ln\frac{q}{\delta}\right.$$

$$\left.+3\delta^2 q-4\delta^3\right)[1-F(q)]^2\frac{dq}{q^4}. \quad (39)$$

The integrals have been evaluated numerically with an IBM card-programmed electronic calculator for the three elements of Table II, and the resulting curves of $\Psi_{12}{}^C$ plotted vs $\mu \equiv \delta/(2\pi/a)$ are shown in Figs. 5 to 9, together with the corresponding one-atom and interference parts. One can see that they lie below the Bethe-Heitler curves, $\Phi_{12}-(4/3)\ln Z$, by approximately 10–20%. The curves for $T=77°$ lie closer to the one-atom curves than the zero-point curves, as the more enhanced temperature vibration brings the substance closer to an amorphous state.

The total cross section is of course given by

$$\sigma_t = \sigma_t{}^C+\sigma_t{}^i. \quad (40)$$

IV. INTERFERENCE PART OF THE CROSS SECTION

The first term of the crystal factor (37) consists of the old Laue-Bragg expression, multiplied by the Debye-Waller factor. This corresponds again to our reciprocal lattice situation of Fig. 1, with the weight of the points reduced with increasing distance from the origin. For $A \sim 100$, the reciprocal lattice points are washed out for $q \gtrsim 10^{-1}$, or outside a distance of 10–15 points. This shows that considerable interference remains, the more so as the maximally contributing values of q given by the screening radius (due to the factor $[1-F(q)]^2/q^4$ in the cross section) are always a good deal below $\sim 10^{-1}$. The continuous part of (37) increases with q as the interference part decreases.

To get the interference part of the cross section, we can take over the "ideal crystal" formulas (23) and (33) and simply insert the Debye-Waller factor $\exp(-Aq^2)$ into the integrand. Because of this factor, we can now radically simplify the integrand, since values of $q \gtrsim 10^{-1}$ will be of no importance. Expressions like $q_\perp^2/2\epsilon_+$ in the roots can be considered small compared to q_z, and the roots expanded. We can then represent the interference cross section in a similar form as the one-atom cross section, namely, as

$$\sigma_{t,\,pair}{}^i = N\frac{Z^2}{137}\left(\frac{e^2}{mc^2}\right)^2\frac{d\epsilon_+}{k^3}$$

$$\times\left[(\epsilon_+{}^2+\epsilon_-{}^2)\sum_{h\geqslant 0}\Psi_1{}^h(\delta,\theta)+\tfrac{2}{3}\epsilon_+\epsilon_-\sum_{h\geqslant 0}\Psi_2{}^h(\delta,\theta)\right], \quad (41)$$

$$\sigma_{t,\,br}{}^i = N\frac{Z^2}{137}\left(\frac{e^2}{mc^2}\right)^2\frac{dk}{k\epsilon_1{}^2}$$

$$\times\left[(\epsilon_1{}^2+\epsilon_2{}^2)\sum_{h\geqslant 0}\Psi_1{}^h(\delta,\theta)-\tfrac{2}{3}\epsilon_1\epsilon_2\sum_{h\geqslant 0}\Psi_2{}^h(\delta,\theta)\right]. \quad (41')$$

The $\Psi_{12}{}^h$ are the same for bremsstrahlung and pair production (with the respective δ's); they are

$$\Psi_1{}^h = \frac{8\delta}{a}\int_\delta^\infty\frac{\exp(-Aq^2)q\,dq}{(\beta^{-2}+q^2)^2}$$

$$\times\int_\delta^{'q}\frac{dq_z{}^2}{[\theta^2q^2-(q_z{}^2-2\pi h/a)^2]^{\frac{1}{2}}}\frac{q^2-q_z{}^2}{q_z{}^2},$$

$$\Psi_2{}^h = \frac{48\delta}{a}\int_\delta^\infty\frac{\exp(-Aq^2)}{(\beta^{-2}+q^2)^2} \quad (42)$$

$$\times\int_\delta^{'q}\frac{dq_z{}^2}{[\theta^2q^2-(q_z-2\pi h/a)^2]^{\frac{1}{2}}}\frac{q^2-q_z{}^2}{q_z{}^4}\delta(q_z-\delta).$$

The variable q has been used instead of $q_\perp^2$. The terms $h<0$ contribute a negligible amount, and have been omitted. This can be seen as follows. Because we must include only regions of real lattice square root, the integrand will be $\neq 0$ only if

$$\frac{2\pi}{a}h+\theta q\geqslant\delta \quad\text{or}\quad q\geqslant\frac{1}{\theta}\left(\delta+\frac{2\pi}{a}|h|\right). \quad (43)$$
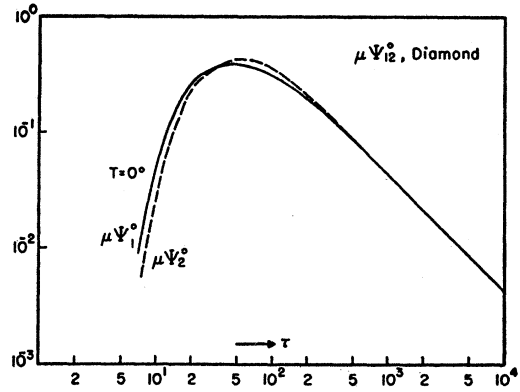

FIG. 3. $\mu\Psi_{12}{}^0$ for diamond.

The most favorable case is $h=-1$, $\delta=0$. Inserting for the largest value considered in the following numerical evaluation, $\theta\sim 5\times 10^{-2}$, and using $(2\pi/a)\sim 7\times 10^{-3}$, we obtain $q\geqslant 1.4\times 10^{-1}$; but these q values give a negligible contribution due to the Debye-Waller factor.

According to the $q_z{}^{-2}$ or $q_z{}^{-3}$ dependence of (42), most contribution comes from q_z values near δ. The lattice root demands

$$\frac{2\pi}{a}h-\theta q\leqslant q_z\leqslant\frac{2\pi}{a}h+\theta q;$$

so for $h=0$, q_z reaches the minimum δ; for $h=0$, it will in general not because of the small angles $\theta\lesssim 10^{-2}$. This shows the minor importance of terms $h=0$. Figure 1 makes this obvious: for small δ and θ, only the plane $h=0$ will contribute a good number of points to the pancake.

Considering $h=0$, and integrating over q_z, we obtain

$$\Psi_1{}^0(\tau) = \frac{4}{\pi\mu}\int_{1/\tau}^\infty\frac{\exp(-Aq^2)q^3dq}{(\beta^{-2}+q^2)^2}\frac{(\tau^2q^2-1)^{\frac{1}{2}}}{\tau^2q^2},$$

$$\Psi_2{}^0(\tau) = \frac{12}{\pi\mu}\int_{1/\tau}^\infty\frac{\exp(-Aq^2)q^3dq}{(\beta^{-2}+q^2)^2}\frac{1}{\tau^3q^3} \quad (44)$$

$$\times\left\{\ln[\tau q+(\tau^2q^2-1)^{\frac{1}{2}}]+\frac{\tau^2q^2-4}{3\tau q}(\tau^2q^2-1)^{\frac{1}{2}}\right\}.$$
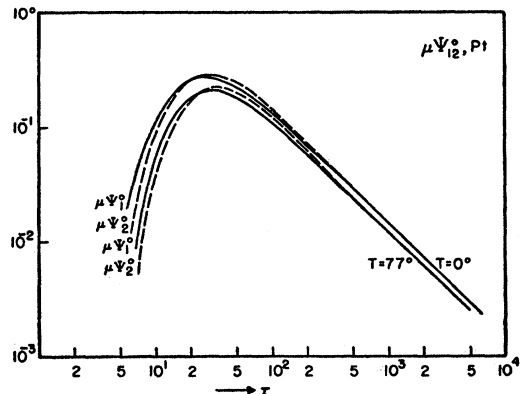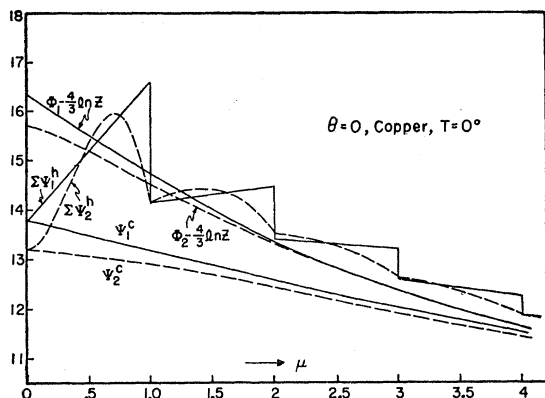

FIG. 4. $\mu\Psi_{12}{}^0$ for Pt.

FIG. 5. Bethe-Heitler ($\Phi_{12}-(4/3)\ln Z$), continuous ($\Psi_{12}{}^C$), and interference functions ($\sum_h\Psi_{12}{}^h$ for $\theta=0$) vs $\mu=\delta/(2\pi/a)$. $\sum_h\Psi_{12}{}^h$ is plotted from the $\Psi_{12}{}^C$ curve upward. Cu, $T=0°$.

The $\Psi_{12}{}^0$ are functions of $\tau=\theta/\delta$ only. They were evaluated numerically for Cu, diamond and Pt at $T=0°$, and for Cu and Pt at $T=77°$ (diamond has nearly no change with temperature). Curves of $\mu\Psi_{12}{}^0$ are plotted vs τ in Figs. 2 to 4. They show a maximum at $\tau\lesssim a_{\text{screen}}$ and decrease above it with a 45° slope in logarithmic scale, meaning proportionality with μ. We read off: for given δ (given primary energy and spectral component), the $h=0$ part of the interference cross section has a maximum at $\theta\lesssim\delta a_{\text{screen}}$, and goes to zero on both sides. Typical δ's are $1/k$ or $1/\epsilon_1$, so the angle of the maximum will be small $\lesssim10^{-2}$, but will be larger than the intrinsic bremsstrahlung and pair production angle mc^2/E by a factor $\sim(a_{\text{screen}}/\lambda_C)$. Because of the factor $1/\mu$ in (44), the maximum will be larger for smaller μ (higher primary energy or lower spectral component), and will be shifted to smaller θ's. Eventually, the maximum would go to infinity, with the corresponding θ going to zero, if at a given primary energy we approach the low end of the bremsstrahlung spectrum (μ or $\delta\to0$). Such values of δ are excluded, however, as our theory is valid only for quanta $\gg mc^2$. In pair production, this phenomenon cannot occur, as δ has a minimum $2/k$ (for equal energy distribution of the pair).
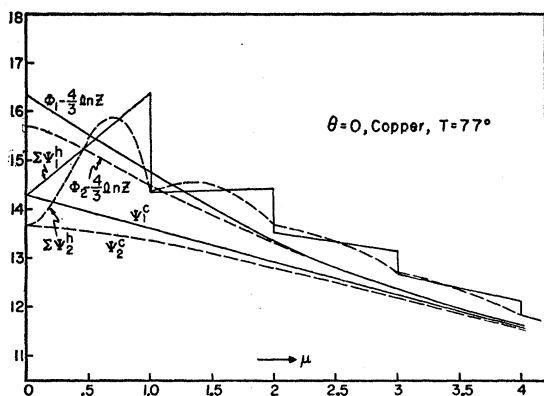

FIG. 6. $\Phi_{12}-(4/3)\ln Z$, $\Psi_{12}{}^C$, and $\sum_h\Psi_{12}{}^h$ for Cu, $T=77°$.

For $h\geqslant1$, the integrals over q_z were done analytically, over q numerically. The $\Psi_{12}{}^h(h\geqslant1)$ depend on δ and θ separately. They simplify for $\theta=0$: here we get contributions from $q_z=(2\pi/a)h$ only, according to (43). The terms in the sum decrease at least as rapidly as h^{-2}, so we need to keep only few of them, such that $(2\pi/a)^2h^2\ll\beta^{-2}$, and can write

$$\sum_{h>0}\Psi_1{}^h(\delta,0)=4\mu U\sum_h\frac{1}{h^2}\exp\left[-A\left(\frac{2\pi}{a}\right)^2h^2\right],$$

$$\sum_{h>0}\Psi_2{}^h(\delta,0)=16\mu^2U\sum_h\frac{h-\mu}{h^4}\exp\left[-A\left(\frac{2\pi}{a}\right)^2h^2\right],$$

(45)

with

$$U=\int_0^\infty\frac{x^3dx}{(\beta^{-2}+x^2)^2}\exp(-Ax^2).$$

The summation has to start from $h\geqslant\mu$, because of the lower limit of the q_z integration. For fixed h and increasing μ, the terms with an h which is being passed
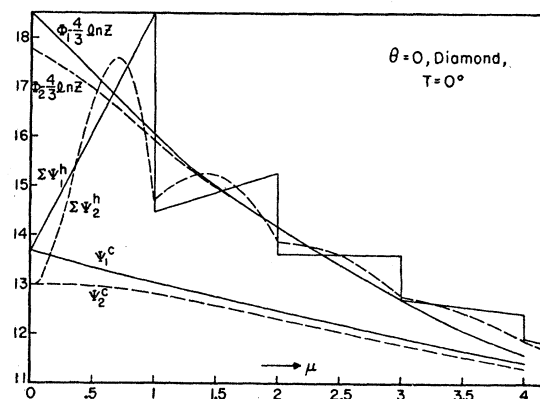

FIG. 7. $\Phi_{12}-(4/3)\ln Z$, $\Psi_{12}{}^C$, and $\sum_h\Psi_{12}{}^h$ for diamond, $T=0°$.

by the μ will drop from the sum; so $\sum\Psi_1$ will be discontinuous in μ, but not $\sum\Psi_2$, because of its factor $(h-\mu)$.

Equation (45) was evaluated numerically, and the results added to the corresponding $\Psi_{12}{}^C$ in Figs. 5 to 9. We see that the curve of continuous plus interference term oscillates around the corresponding Bethe-Heitler curve. A numerical investigation was made for Cu at $T=0$ to find the behavior of $\sum\Psi_{12}{}^h$ for angles $\theta\neq0$. We merely quote the result. The discontinuities get rounded off and become flatter when θ increases. At $\theta\sim2\times10^{-2}$, about half of the excess above the one-atom curve is removed, and for $\theta\sim5\times10^{-2}$, the peaks have gone over rather smoothly into the one-atom curve.

V. RESULTS

From (39), (41), and (41'), we have calculated the bremsstrahlung spectrum and the pair energy distribution for copper at $T=0$. The bremsstrahlung spectrum is plotted in Fig. 10 for 200 Mev and in Fig. 11 for 1 Bev, together with the angular dependence of selected spectral components. The big enhancement over the
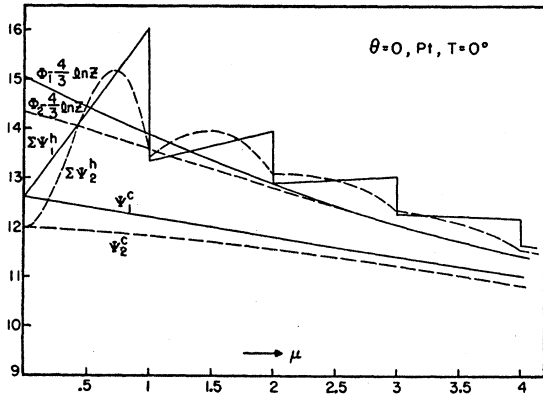
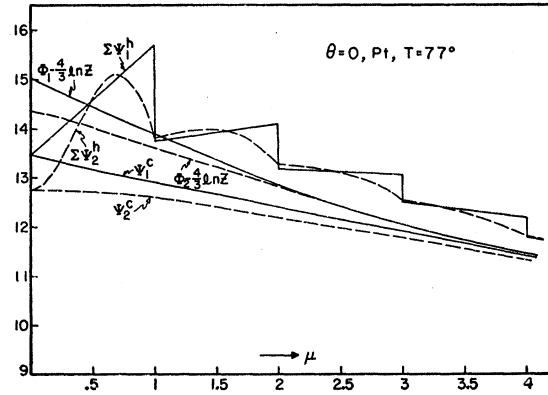FIG. 8. $\Phi_{12}-(4/3)$ ln$Z$, Ψ_{12}^C, and $\Sigma_h\Psi_{12}^h$ for Pt, $T=0°$.

FIG. 9. $\Phi_{12}-4(/3)$ ln$Z$, Ψ_{12}^C, and $\Sigma_h\Psi_{12}^h$ for Pt, $T=77°$.

Bethe-Heitler spectrum at the low-frequency end $(\delta\ll2\pi/a)$ at small angles is due to the $h=0$ part of the cross section. The higher h's (representing the harmonics in the Fourier decomposition of the potential) show themselves as little sharp peaks at the high-frequency end. They decrease with angle, whereas the low-frequency part of the spectrum first increases from its "continuous" value at $\theta=0$ to the above discussed maximum, and then goes down to the Bethe-Heitler spectrum. The softer the radiation, the higher is the maximum, and at the smaller angles it occurs. Lowering the primary energy lowers the $h=0$ enhancement and shifts the $h>0$ peaks to the left.

This behavior can easily be understood from Fig. 1, when one considers that a linear scale in μ, going to ∞, corresponds to an $x=k/\epsilon_1$ scale which converges towards $x=1$. For $\theta=0$, the pancake does not contain the plane $h=0$, and so we have only a contribution from

the noninterference spectrum. Increasing θ tips the pancake and puts more and more points from the $h=0$ plane into it. The optimum θ will be that one for which the maximum of the q distribution, $1/a_{screen}$, coincides with this plane, which occurs at $\theta\sim\delta a_{screen}$. The high-frequency peaks lie at the values $\delta=(2\pi/a)h$.

Energy distributions in pair production are plotted in Fig. 12 for 1 Bev, Fig. 13 for 5 Bev for copper at $T=0°$, together with their angular dependence. At $h=0$, the curve lies below the Bethe-Heitler value, except for the peaks due to $h>0$ at both ends. With increasing angle, the $h=0$ effect enhances the cross section, but tending back to the one-atom cross section for $\theta\sim5\times10^{-2}$. The enhancement is more pronounced the higher the primary energy. For small angles $\lesssim10^{-2}$, we can expect considerable increase of total pair production probability over its complete screening value of 7/9 per radiation length.
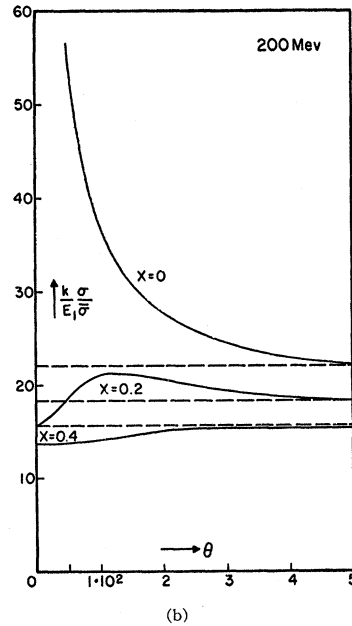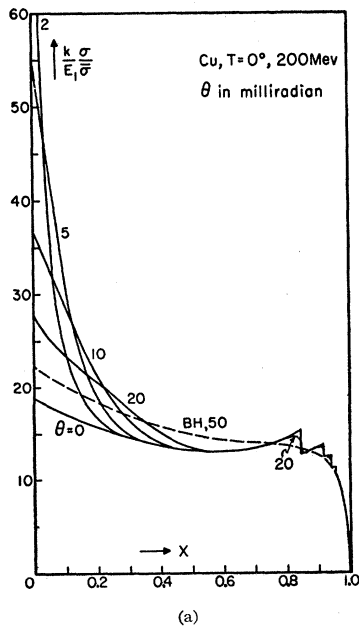

(a)

(b)

FIG. 10. Bremsstrahlung spectrum in a Cu crystal at $T=0°$, $\epsilon_1=200$ Mev in units $\bar{\sigma}=Z^2(e^2/mc^2)^2/137$, and corresponding angular dependence. $x=k/\epsilon_1$.
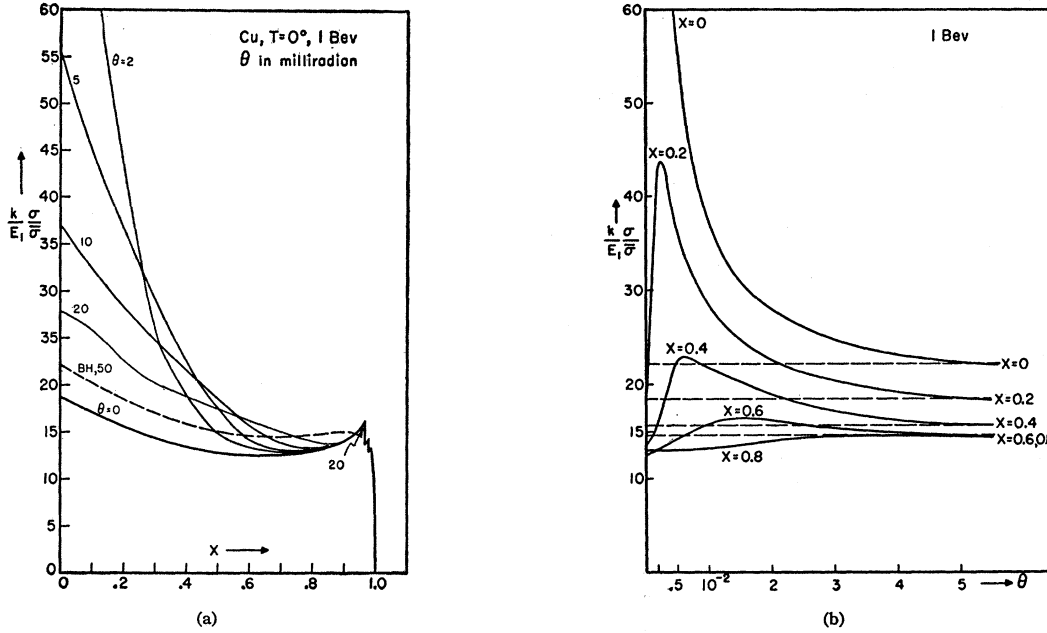
FIG. 11. Bremsstrahlung spectrum in a Cu crystal at $T=0°$, $\epsilon_1=1$ Bev, and angular dependence.

Let us finally consider the case that our cross section in the crystal be averaged over all angles θ. This means that the differential cross section in q space has its pancake shape averaged out and turns into a function which varies slowly over several reciprocal lattice spacings $2\pi/a$. Then, however, we can replace the crystal factor (6) or (38) by its average value over a volume small compared to dimensions over which the function changes appreciably, but containing at least one reciprocal lattice cell $(2\pi)^3/\Delta$. This average is simply

$$\langle |\sum_L \exp[i\mathbf{q}\cdot(\mathbf{L}+\mathbf{u}_L)]|^2\rangle = N, \qquad (46)$$

and we get back the Bethe-Heitler formula. Thus, an average over θ cancels all interference. Situations where this might occur are a crystal powder, or the randomly oriented Ag Br grains in emulsion. Concerning the latter case, one could have hoped to explained the anomalous trident production[15] (direct pair creation by electron impact) by a constructive crystal interference of the process itself, or of the bremsstrahlung via production of pseudotridents by a forward emitted quantum. The cancellation of interference by average over orientations seems to exclude this possibility of explanation.
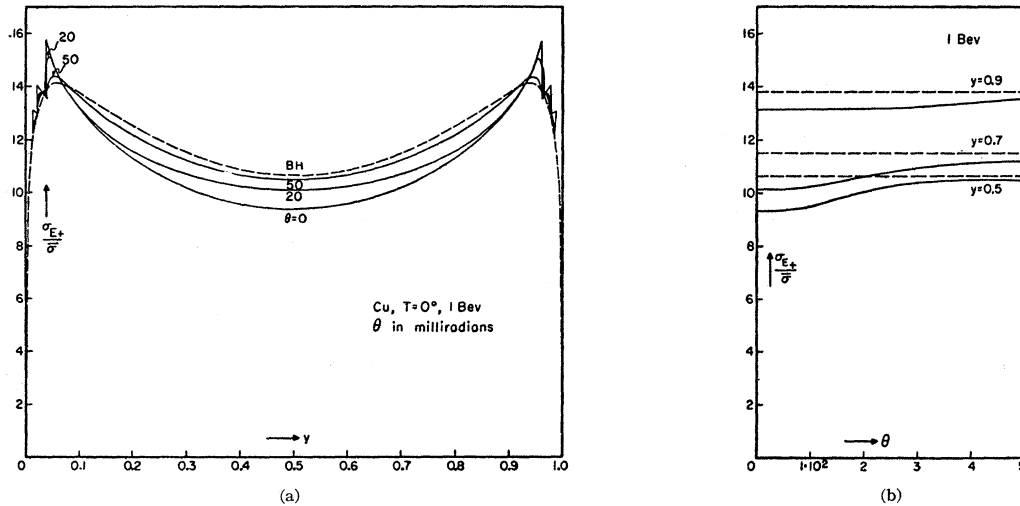

FIG. 12. Pair energy distribution in a Cu crystal at $T=0°$, $k=1$ Bev in units $\bar\sigma=Z^2(e^2/mc^2)^2/137$, and angular dependence. $y=\epsilon_+/k$.

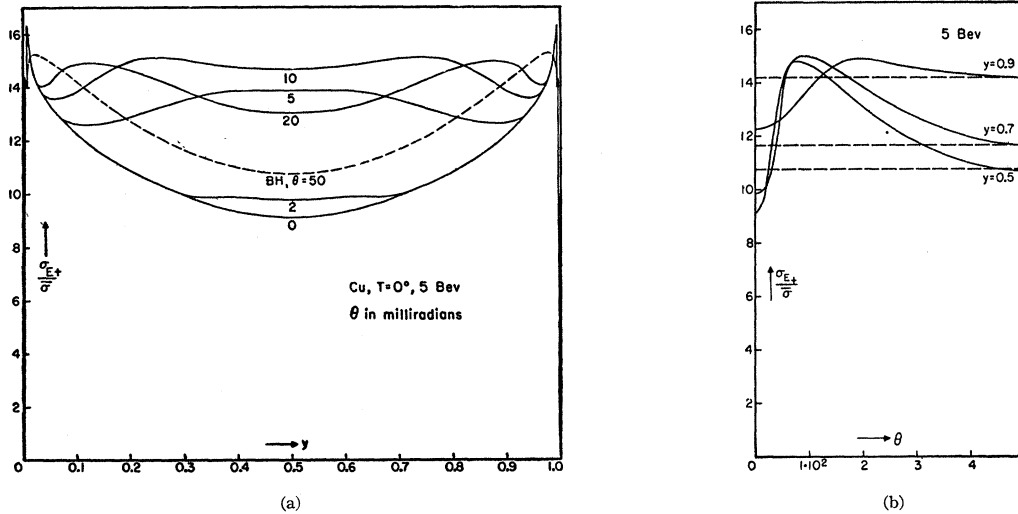[15] M. Koshiba and M. F. Kaplon, Phys. Rev. 100, 327 (1955).

FIG. 13. Pair energy distribution in a Cu crystal at $T=0°$, $\epsilon_1 = 5$ Bev, and angular dependence.

VI. DISCUSSION

Conditions of applicability of the Born approximation are,[7] for bremsstrahlung:

$$2\pi Ze^2/\hbar v_{12} \ll 1, \tag{47}$$

and for pair production:

$$2\pi Ze^2/\hbar v_{\pm} \ll 1, \tag{48}$$

which are satisfied for high energies. A qualitative condition is that the potential times its range shall not be too large, so that an expansion in powers of Ze^2 is possible. Since the crystal potential consists of an array of essentially nonoverlapping atomic potentials, for each of which Born approximation is valid if Eqs. (47) and (48) hold, the Born approximation is valid for our crystal calculation to the same extent as it is valid for the one-atom case.

Experimental verification of the calculated effect is within the range of present-day accelerators. Especially the striking enhancement of the low-frequency end of the bremsstrahlung spectrum will be measurable, for example by observing a low-frequency spectral component and rocking the target crystal through a small angular interval around $\theta = 0$, which would produce a minimum of the observed yield at $\theta = 0$. Also the $h = 1$ peak might be observable, because its rise will persist even to lower energies, and its position get shifted to the left of the spectrum. The target crystal should be thin, $\lesssim 1/1000$ radiation length, in order to prevent multiple scattering of the electrons. For pair production, less precautions are necessary, as electronic and nuclear Compton effect are negligible; however, the effect sets in at much higher energies. It might be reasonable only to look for an increase of the total pair production probability above its one-atom value of $7/9$ per radiation length.

There are possible applications of the effect. In bremsstrahlung, the $h = 1$ peak provides a slight chance for monochronatization of radiation; the big increase is in the low-frequency part and therefore of less use to the experimenter. The θ dependence of the pair cross section could be employed for a collimating mechanism of high-energy γ rays because of the dip at $\theta = 0$ and the steep rise up to $\theta \sim 10^{-2}$ (Fig. 13). Components of the beam traversing the crystal under some small angle will be more strongly absorbed than those traveling along a line of atoms. This could provide a partly collimated beam of considerable lateral width. Similar considerations apply to electron beams also.

ACKNOWLEDGMENTS